

Article

Experimental Research on the Mechanical Properties of Recycled Aggregate Particle Gradation and Addition on Modified Cement Soil

Huaqiang Tao ¹, Beifeng Lv ¹ , Yanting Wu ¹, Mengdan Dai ¹, Yutao Pan ², Na Li ¹ , Wei Wang ¹ 
and Ping Jiang ^{1,*} 

¹ School of Civil Engineering, Shaoxing University, Shaoxing 312000, China; taohqusx@126.com (H.T.); 20020852047@usx.edu.cn (B.L.); 19020852065@usx.edu.cn (Y.W.); 18020852032@usx.edu.cn (M.D.); lina@usx.edu.cn (N.L.); wellswang@usx.edu.cn (W.W.)

² Department of Civil and Environmental Engineering, Norwegian University of Science and Technology, 7491 Trondheim, Norway; yutao.pan@ntnu.no

* Correspondence: jiangping@usx.edu.cn

Abstract: In order to study the effects of recycled aggregate with different particle gradations and different contents on the mechanical properties of cement soil modified by nano-MgO, unconfined compressive strength and scanning electron microscope (SEM) tests were carried out. The cement content was fixed at 15% and the nano-MgO content was 1.5%. The effects of two ages, three recycled aggregate contents, and three recycled aggregate particle gradations were considered. The test results show that the unconfined compressive strength of natural graded (RA), recycled coarse aggregate (SRA), and recycled fine aggregate (TRA) reached the maximum when the content of recycled aggregate was 20%, and the unconfined compressive strength of SRA was higher than that of TRA and RA. The residual strength of RA and SRA samples first increased and then decreased with the increase in recycled aggregate content, and the residual strength of TRA samples increased gradually with the increase in recycled aggregate content. The variation law of peak strain and peak strength of the three particle graded samples was consistent, and the variation law of brittle failure degree was highly consistent with that of residual strength. When the recycled aggregate content of RA, SRA, and TRA samples was 20%, the deformation resistance and stiffness of the samples were the best. In addition, SRA samples showed the best deformation resistance, followed by TRA samples and, finally, RA samples. The smaller the porosity of the sample, the tighter the sample structure and the stronger the bearing capacity of SRA. The unconfined compressive strength of the WPRA sample was represented by an exponentially negative power function of the porosity.

Keywords: recycled aggregate; particle gradation; content; mechanical property



Citation: Tao, H.; Lv, B.; Wu, Y.; Dai, M.; Pan, Y.; Li, N.; Wang, W.; Jiang, P. Experimental Research on the Mechanical Properties of Recycled Aggregate Particle Gradation and Addition on Modified Cement Soil. *Crystals* **2022**, *12*, 428. <https://doi.org/10.3390/cryst12030428>

Academic Editors: Umberto Prisco and Per-Lennart Larsson

Received: 23 February 2022

Accepted: 17 March 2022

Published: 19 March 2022

Publisher's Note: MDPI stays neutral with regard to jurisdictional claims in published maps and institutional affiliations.



Copyright: © 2022 by the authors. Licensee MDPI, Basel, Switzerland. This article is an open access article distributed under the terms and conditions of the Creative Commons Attribution (CC BY) license (<https://creativecommons.org/licenses/by/4.0/>).

1. Introduction

A large quantity of soft soil is distributed in coastal areas. This soil has the disadvantages of large compression and poor bearing performance. In practical engineering, this results in a series of problems, such as insufficient strength or large deformation. Therefore, certain reinforcement measures need to be implemented to improve the bearing capacity of the soft soil layer, and thus meet the engineering requirements [1–3]. As a result of the rapid development of the social economy and continuous advancement of urbanization, the civil engineering industry has also flourished, which has led to a serious shortage of construction resources. At the same time, the demolition of old buildings produces a large amount of construction waste, which poses a huge challenge to the ecological environment [4,5]. There is also an urgent need to find ways to rationally utilize the construction waste. Therefore, the recycling of aggregates has emerged [6]. The concrete produced by the demolition of waste buildings is subjected to a series of treatments, such as crushing and screening, and

the final recycled aggregate is reused as a building material in the construction process. This provides a promising solution for saving natural resources, protecting the ecological environment, and reducing the accumulation of construction waste, and fully implements the concept of sustainable development [7–9].

Particle gradation is one of the important factors affecting the mechanical properties of soil. A large number of studies have found that particle gradation has obvious effects on the compressive strength, tensile strength, shear strength, permeability, and rheological properties of soil [10–12]. Chian et al. [13] conducted unconfined compressive strength tests on coarse-sand clay, fine-sand clay, and well-graded clay samples to study the effect of sand impurity particle gradation on the strength characteristics of cement-treated clay. The test results showed that the strength of the coarse-sand clay samples is lower than that of the fine-sand clay samples, but the cement hydration process of the coarse-sand clay samples is faster than that of the fine-sand clay and well-graded clay samples. The strength of the fine-sand clay samples is slightly higher than that of the well-graded clay samples in the low-strength range, but slightly lower in the high-strength range over 1500 kPa. In order to study the effect of particle gradation on the cyclic shear performance of recycled concrete aggregate (RCA), Huang et al. [14] carried out monotonic direct shear, cyclic direct shear, and post-cycle monotonic direct shear tests on RCA samples with different particle gradations. The test results showed that the shear strength of the well-graded RCA samples was the largest. Under different normal stresses and shear displacements, the shear strength of the well-graded RCA samples was significantly larger than that of other RCA types, and the hysteresis curve area was also the largest. Under the influence of particle gradation, the shear stiffness and damping ratio of the well-graded RCA samples were the largest, and the shear stiffness of the discontinuously graded RCA samples was between those of the well-graded and poorly-graded RCA samples. The damping ratio of the poorly-graded RCA samples was between those of the well-graded and discontinuously graded RCA samples. The shear strength of RCA samples was improved after cyclic shearing, and the well-graded RCA samples exhibited the best friction characteristics. Ren et al. [15] studied the effect of particle gradation on the permeability of calcareous sand through the traditional indoor constant head seepage test. The test results showed that the particle gradation of calcareous sand had a certain influence on its permeability; specifically, when the non-uniformity and curvature coefficients were controlled as a single variable, the permeability coefficient of the calcareous sand samples increased gradually with the increase in the non-uniformity and curvature coefficients of the calcareous sand particle size. In order to study the effect of particle gradation on the mechanical properties of machine-made sand concrete, Xie et al. [16] carried out a series of mechanical tests on five kinds of machine-made sands with different particle gradations, namely, the slump test, cube compressive strength test, axial compressive strength test, splitting tensile strength test, and elastic modulus test. The test results showed that with the increase in coarse particles having a particle size of 1.18–4.75 mm in the particle gradation of machine-made sand, the slump value, cubic compressive strength, axial compressive strength, splitting tensile strength, and elastic modulus of machine-made sand concrete showed a trend of first increasing and then decreasing. When the fineness modulus of machine-made sand was 2.90, the mechanical properties of machine-made sand concrete were optimal, and were also greatly improved compared with those of natural sand concrete. In order to study the effect of aggregate particle size on the mechanical properties of recycled aggregate concrete (RAC), Duan et al. [17] carried out a series of hardening density, compressive strength, split tensile strength, and chloride salt corrosion resistance tests. The test results show that optimizing the particle gradation of the aggregate can comprehensively improve the performance of RAC, which can effectively improve its hardening density, compressive strength, and splitting tensile strength, thus improving its durability. In summary, a large number of research results [18–21] show that particle gradation has an important effect on the performance of various building materials. Good particle gradation can

effectively improve the mechanical properties of materials, and improve their permeability and durability.

At present, a large number of research results show that particle gradation plays an important role in the mechanical properties of building materials such as sand, clay and recycled concrete aggregate. The research content of this study was not aimed at the mechanical properties of the material itself due to the factor of particle gradation, but focused on the recycled aggregate as an admixture to study the influence of its particle gradation on the mechanical properties of other base materials. This type of research is relatively rare at present. Therefore, using soft soil as a base, in this study, recycled aggregates having different contents and particle gradations were added to study their improvement effect on the mechanical properties of the soft soil, so as to obtain the best content and particle gradation of recycled aggregate. The research results of this study can be applied to the reinforcement of soft soil foundations, and to improving the properties of soft soil with poor performance, so as to meet the requirements of engineering construction and provide a new means for the application of recycled aggregate to realize the recycling of resources.

2. Test Materials and Methods

2.1. Test Materials

The soft soil used in this test was collected from an industrial area in Shaoxing, and the overall appearance was yellowish-brown. Its basic physical properties are shown in Table 1.

Table 1. Physical properties of soft soil in an industrial area of Shaoxing.

Physical Index	Porosity	Liquid Limit/%	Plastic Limit/%	Liquid Index	Plastic Index
Index value	1.74	44	30	0.23	13.5

P.O32.5 Portland cement produced by Shangyu Conch Cement Co., Ltd. (Shaoxing, China), was used throughout the test, which conformed to the GB175-2007 implementation standard. The color was gray-brown, and its specific chemical composition is shown in Table 2.

Table 2. Main chemical composition of cement.

Composition	S _i O ₂	Al ₂ O ₃	Fe ₂ O ₃	MgO	SO ₃	K ₂ O	Na ₂ O	Mn ₂ O ₃	CaO
Content/%	20.59	4.90	3.40	2.51	2.07	0.5	0.7	0.4	65.10

Nano-MgO was produced by Maclean Co., Ltd. (Shanghai, China) and had an average particle size of 50 nm and high purity. It is white spherical powder and its basic parameters are shown in Table 3.

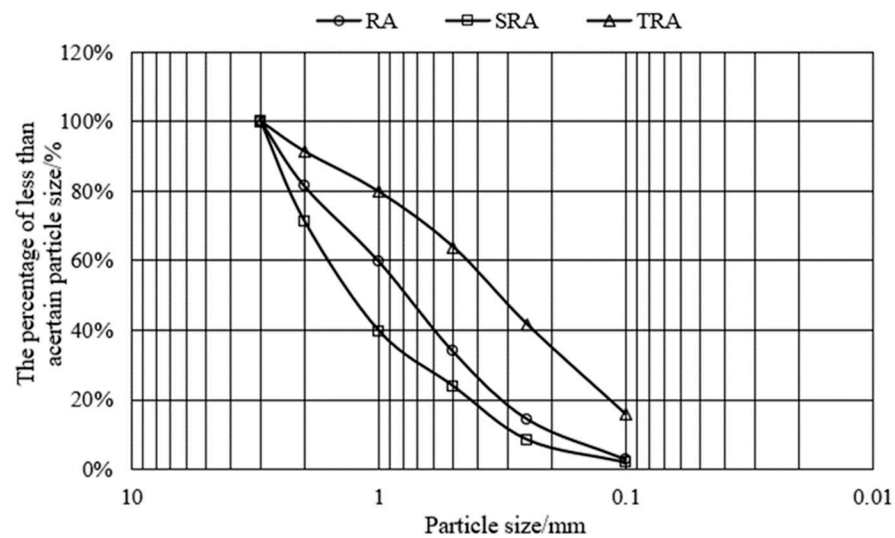
Table 3. Basic parameters of nano-MgO.

Composition	MgO	Cl	Mn	K	Na	Ca	Fe
Content/%	99.8	0.10	0.021	0.016	0.012	0.16	0.002

The recycled aggregate was taken from the waste concrete of a demolition site in Shaoxing and produced by Shanghai Youhong Environmental Technology Co., Ltd. (Shanghai, China). The maximum particle size was less than 10 mm, and most particles were round and granular having a blue-gray color. In order to study the effect of recycled aggregates' particle gradation, by referring to the particle sieving curve of Peng Wan [22], two additional recycled aggregates with different particle gradations were designed as test materials on the basis of natural gradation. The mass fraction of each particle size is shown in Table 4 and Figure 1.

Table 4. Mass fraction of recycled aggregates of different grades under each particle size.

Mass Fraction/%	Particle Size D/mm					
	$3 \geq D \geq 2$	$2 \geq D \geq 1$	$1 \geq D \geq 0.5$	$0.5 \geq D \geq 0.25$	$0.25 \geq D \geq 0.1$	$D \leq 0.1$
RA	18.6	21.6	25.9	19.4	11.5	3.0
SRA	28.6	31.6	15.9	15.5	6.5	1.9
TRA	8.6	11.6	15.9	22.4	25.8	15.7

**Figure 1.** The particle gradation curve of the recycled aggregate.

2.2. Test Scheme

The recycled aggregate with different contents (10%, 20%, 30%) and three particle gradations (RA, SRA, TRA), cement with the mixing ratio of 15%, and nano-MgO with the mixing ratio of 1.5%, were added to soft soil and cured for 7 and 28 d, respectively. When the samples reached the curing age, unconfined compressive strength tests were carried out. The specific scheme is shown in Table 5.

Table 5. Test scheme.

Particle Gradation	Sample No.	Cement Content/%	Moisture Content/%	Nano-MgO Content/%	Recycled Aggregate Content/%	Curing Age/d
Natural gradation (RA)	RA-10	15	30	1.5	10	7, 28
	RA-20				20	
	RA-30				30	
Recycled coarse aggregate (SRA)	SRA-10	15	30	1.5	10	7, 28
	SRA-20				20	
	SRA-30				30	
Recycled fine aggregate (TRA)	TRA-10	15	30	1.5	10	7, 28
	TRA-20				20	
	TRA-30				30	

2.3. Sample Preparation

According to the Standard for Geotechnical Test Methods (GBT 50123-2019) [23], the sample preparation process can be divided into the following steps, and the specific process is shown in Figure 2:

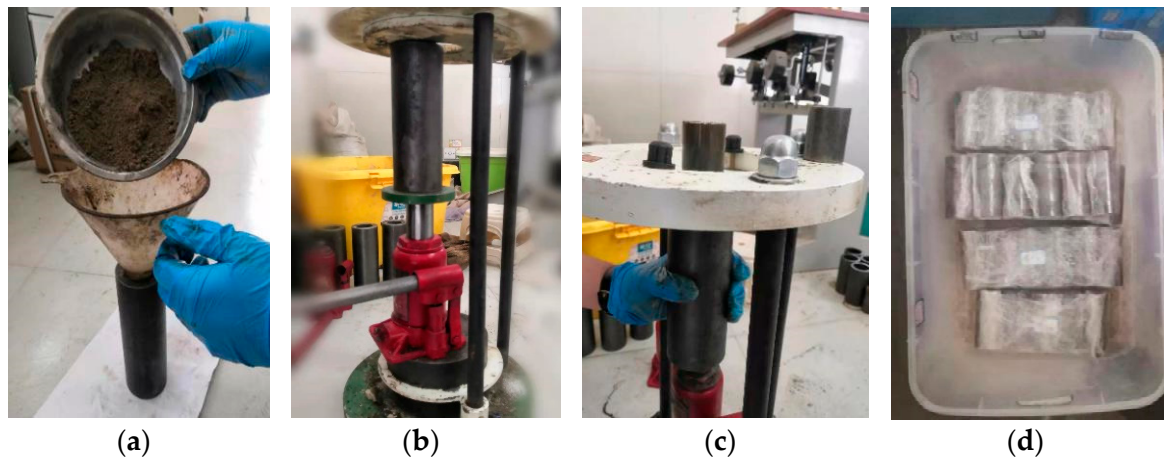


Figure 2. Sample preparation process: (a) filling; (b) standing; (c) demolding; (d) curing.

First, the soft soil and recycled aggregates required for the test were placed into a constant temperature oven for 24 h to ensure that they were completely dry. According to the mixing ratio designed in the test scheme, a certain mass of soft soil, recycled aggregate, cement, nano-MgO, and water was weighed, and then mixed and stirred evenly. The mixed mixture was poured into the sample preparation mold evenly in three stages and compacted completely. In addition, it was allowed to stand for 10 min after each compaction to prevent rebounding. The compacted mixture was demolded to obtain a cylindrical sample having a diameter of 39.1 mm and a height of 80 mm. Then, the samples were wrapped with film to maintain their freshness and placed into a standard curing box for curing. The curing time was 7 and 28 d.

2.4. Test Equipment and Methods

A fully automatic unconfined compressive strength tester produced by Nanjing TKA Co., Ltd. (Nanjing, China), was adopted for the unconfined compressive strength test, and the compression rate was set to 1 mm/min. According to the Standard for Geotechnical Test Methods (GBT 50123-2019) [23], when the axial force reaches the peak value or reaches stability, the test can be stopped by applying 3–5% axial strain on the basis of the failure strain.

A tungsten filament high and low vacuum scanning electron microscope (model JSM-6360LV) produced by JEOL Ltd. (Tokyo, Japan), was used in the test. First, after the sample preparation was completed, a crystal spraying operation was performed to ensure that the sample had sufficient conductivity. Then, the sample was placed in the test bench, and the height of the lens was adjusted. Finally, images under different magnifications were taken.

3. Results and Analysis

3.1. Stress–Strain Curve

Due to the contingency and error of the unconfined compressive strength test, the results obtained by only one test are not representative or repeatable. In order to reduce the data discretization caused by test errors, five repeated tests were carried out on the samples with the same mixing ratio, and the normalization curve of five groups of test data was obtained after normalization using the weighted average, as shown in Figure 3. Figure 4 shows the stress–strain curves of recycled aggregates with different contents and three particle gradations at 7 and 28 d.

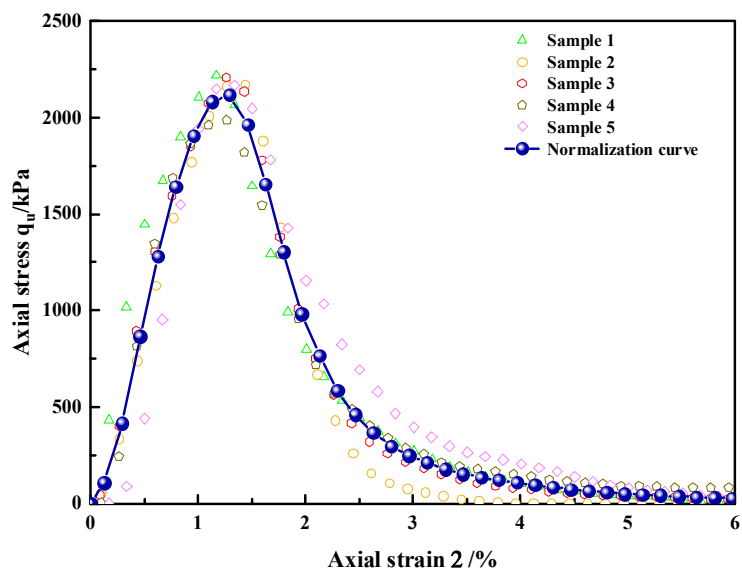


Figure 3. Typical stress–strain normalization curve of RA-10-7d.

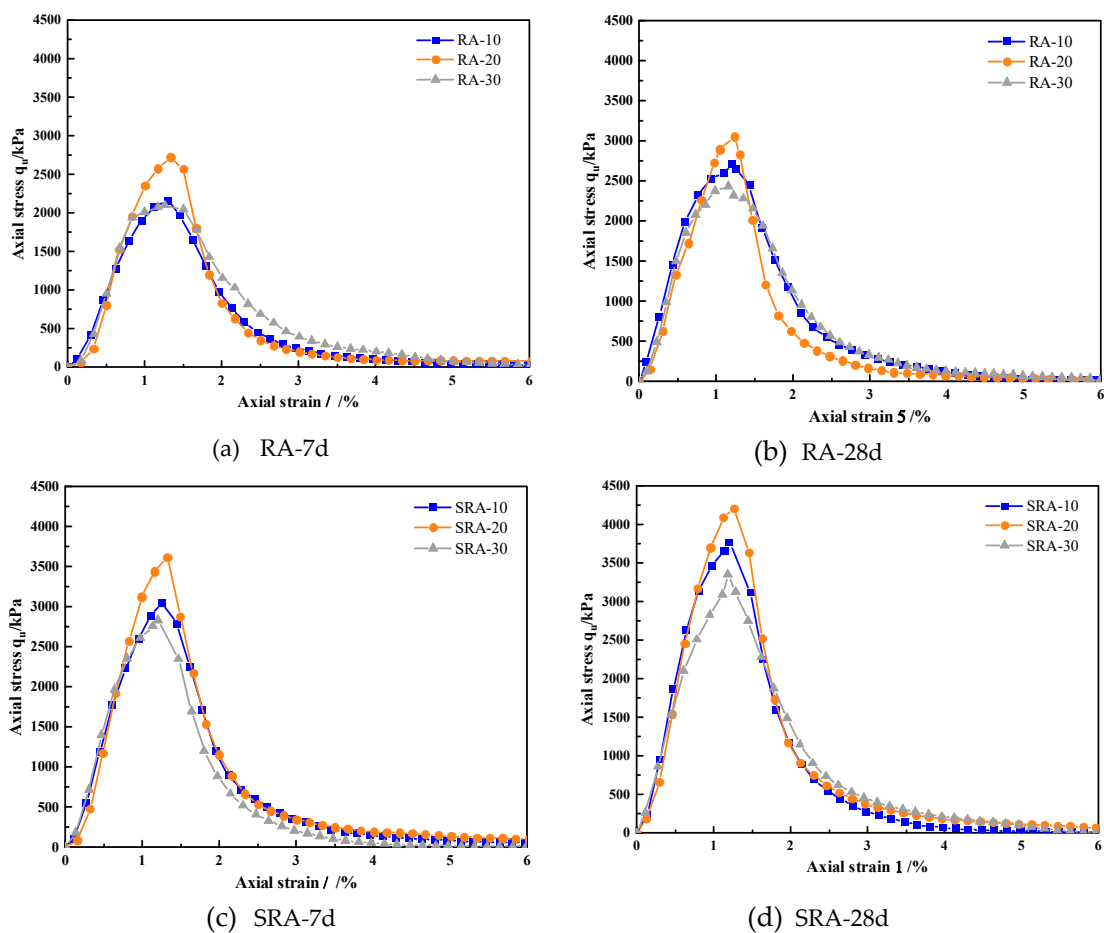


Figure 4. Cont.

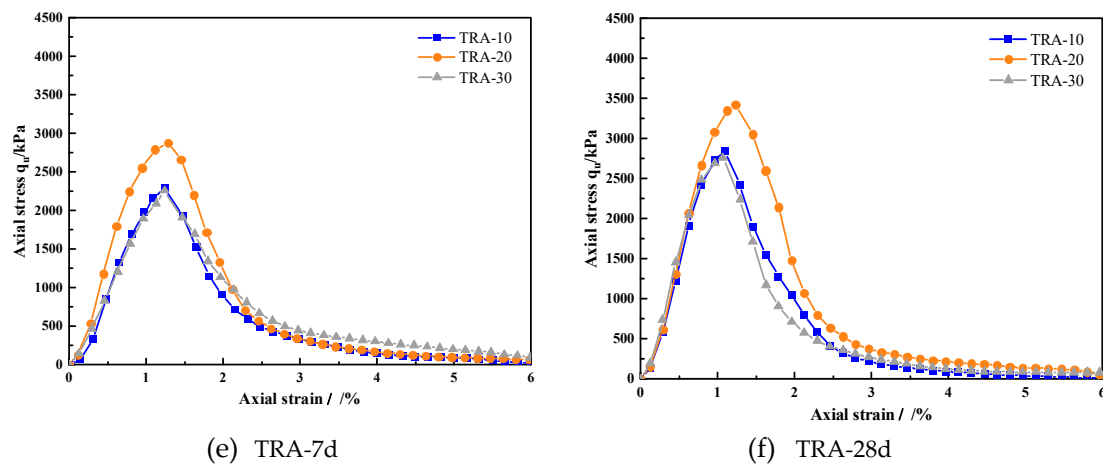


Figure 4. Stress–strain relationship curve of samples with different particle grading recycled aggregate contents: (a) RA-7d; (b) RA-28d; (c) SRA-7d; (d) SRA-28d; (e) TRA-7d; (f) TRA-28d.

Figure 4 shows that the stress–strain curves of all samples have a hump shape, and the stress–strain curves of samples with different recycled sand contents and different particle gradations basically show the same change law; that is, the stress first increases and then decreases with the increase in strain, representing softening curves. These stress–strain curves can be roughly divided into three stages of development: (1) The elastic deformation stage (strain is 0%–1%). The specific performance is that the slope of the stress–strain curve increases, and the stress increases almost linearly with the strain. The soil particles in the sample were compressed by the applied stress, but did not fail. (2) The development stage of plastic deformation (strain is 1%–1.5%). The curve begins to deviate from the straight line at this stage, and the stress growth is not obvious. At this time, due to the continuous increase in the pressure, the structure of the soil particles began to be destroyed, the gaps between the particles were continuously compacted, and micro-cracks appeared in the sample. (3) The softening stage (strain is 1.5%–6%). When the stress exceeds the peak value, the stress gradually decreases with the continuous increase in the strain. At about 3% to 5% greater than the strain of the peak strength, the curve begins to flatten out and maintains a certain residual strength. At this stage, the cracks in the sample gradually expand and extend until the sample cracks and fails. Further analysis found that the change in the stress–strain curve at the age of 7 d is slower than that at the age of 28 d. Among the three particle grading samples, the stress–strain curve of the SRA sample is the steepest, TRA is second, and RA is the slowest.

3.2. Peak Strength

The unconfined compressive strength can be obtained from the stress–strain relationship curve of samples with different particle grading recycled aggregate contents, and the change curve of the unconfined compressive strength is plotted in Figure 5.

Figure 5 shows that the unconfined compressive strength of each sample at 28 d is significantly higher than that at 7 d with the same particle gradation. When the recycled aggregate content is 10%, 20%, or 30%, the unconfined compressive strength of RA-28d sample increased by 25.9%, 12.2%, or 14.6%, respectively, compared with that of the RA-7d sample under natural gradation. Under the recycled coarse aggregate gradation, the unconfined compressive strength of the SRA-28d sample increased by 23.6%, 16.4%, and 18.3%, compared with that of SRA-7d sample, respectively. Under the recycled fine aggregate gradation, the unconfined compressive strength of the TRA-28d sample increased by 24.5%, 18.9%, and 22.1% compared with that of TRA-7d sample, respectively. It was found that when the recycled aggregate content is 10% under the three levels of particle gradation, the unconfined compressive strength of the 28 d samples increased the most

compared with that of the 7d samples, followed by the 30% content and, finally, the 20% content.

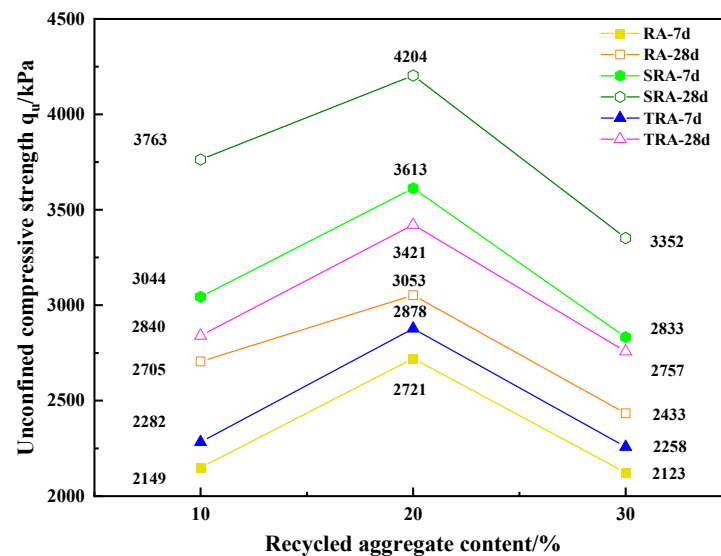


Figure 5. Change curve of unconfined compressive strength of samples with different particle grading recycled aggregate contents.

At 7 and 28 d, the unconfined compressive strengths of RA, SRA, and TRA samples first increased and then decreased with the increase in recycled aggregate content. The maximum unconfined compressive strength was reached when the recycled aggregate content was 20%, and minimum was reached when the recycled aggregate content was 30%. When the recycled aggregate content was 20%, the unconfined compressive strengths of RA-7d and RA-28d samples reached 2721 and 3053 kPa, respectively, which were 25.6% and 12.9% higher than those having recycled aggregate content of 10%. The unconfined compressive strengths of SRA-7d and SRA-28d samples reached 3613 and 4204 kPa, respectively, which were 18.7% and 11.7% higher than having with recycled aggregate content of 10%. The unconfined compressive strengths of TRA-7d and TRA-28d samples reached 2878 and 3421 kPa, respectively, which were 26.1% and 20.5% higher than those having recycled aggregate content of 10%. It can be found through the analysis that the recycled aggregate content has a great influence on the unconfined compressive strength of samples, which is also consistent with the research results obtained by Li Yugen, Li Fang et al. [24,25]. There are a large number of clay particles in soft soil. Adding an appropriate quantity of recycled aggregates to soft soil can improve the particle gradation of the soil. During cement hydration and the nano-MgO pozzolan reaction, a large amount of cement is produced, which effectively bonds soft soil with recycled aggregate. This provides the skeleton force for the soft soil, thereby further improving the bearing capacity of the cement soil. However, when an excessive amount of recycled aggregate is added to cement soil, the contact area between the recycled aggregate and soft soil increases greatly, and the quantitative cement and nano-MgO cannot fully contact the recycled aggregate. Thus, the provided cementing force is too low, resulting in a low level of cohesion between the soil bodies and a downward trend in the strength of the cement soil. Therefore, in actual construction projects, it is necessary to strictly control the recycled aggregate content in cement soil to achieve the optimal application effect.

By comparing the unconfined compressive strength of samples under three particle gradations, it was found that the unconfined compressive strength of SRA samples was highest at 7 and 28 d, followed by that of the TRA samples and, finally, that of the RA samples. By analyzing the law of unconfined compressive strength of SRA, TRA and RA samples, it was found that, at the same curing age and with the same recycled aggregate content, the unconfined compressive strength of SRA samples was stable, and between

20% and 30% higher than that of TRA samples, and between 30% and 40% higher than that of RA samples. With the same recycled aggregate content, SRA samples contain more coarse particles, among which, the brick and concrete particles having larger sizes can provide a good skeleton force in the soil structure, thus enhancing the rigidity of the cement soil so as to maximize the soil's bearing capacity. TRA samples contain a large number of fine particles. In addition to the skeleton force provided by a small quantity of recycled aggregates having a large particle size, the fine particles can fill a large number of large pores between the coarse particles, making the soil structure more compact. Therefore, the strength of cement soil under this particle gradation was second only to that of SRA samples. Finally, the recycled aggregate content under different particle gradations in RA samples was close to the average level, and the boundary between the coarse and fine particles was less obvious, and thus had a limited effect. Therefore, compared with SRA and TRA samples, RA samples had a poor effect on the increase in the compressive strength of cement soil.

3.3. Residual Strength

Residual strength is one of the important physical and mechanical properties, and refers to the residual ability of soil to resist external loads after macroscopic failure; it can be obtained from the stress–strain curve throughout the whole process. [26,27]. According to the “Standards for Geotechnical Test Methods” (GBT 50123-2019) [23], the maximum strain of the unconfined compressive strength test is generally taken as the peak strain plus 3%–5%, and the peak strain of this test is kept between 1%–2%, so the maximum strain range of the test is 4%–7%. The residual strength in this study was defined as the stress value corresponding to the strain of 6% on the stress–strain curve, as plotted in Figure 6.

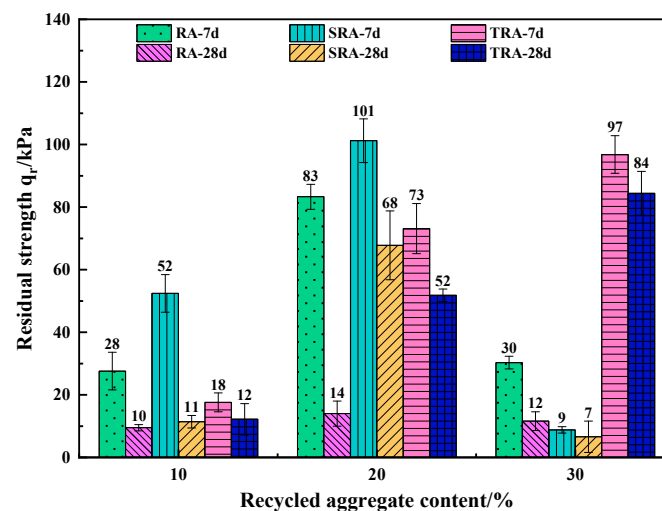


Figure 6. Residual strength of recycled aggregate samples with different particle gradations.

Figure 6 shows that the residual strength of samples with different recycled aggregate contents under three particle gradations is higher at 7 d than that at 28 d. When the recycled aggregate content is 20%, the residual strength of the SRA-7d sample is the largest, reaching 101 kPa, which is 48.5% higher than that of the SRA-28d sample. Comparing the variation law of the residual strength of samples with different recycled aggregate contents under three particle gradations, the residual strengths of RA and SRA samples first increase and then decrease with the increase in recycled aggregate content. When the recycled aggregate content is 20%, the maximum value is reached. Compared with 10% content, the residual strength of RA-7d, RA-28d, SRA-7d, and SRA-28d samples is increased by 196.4%, 40%, 94.2%, and 518.2%, respectively, when the recycled aggregate content is 20%. The residual strength of TRA samples increases gradually with the increase in recycled aggregate content, and reaches the maximum value with 30% content. Compared with 10%

content, the residual strength of TRA-7d and TRA-28d samples is increased by 438.9% and 600.0%, respectively. Compared with 20% content, the residual strength of TRA-7d and TRA-28d samples is increased by 32.9% and 61.5%, respectively.

3.4. Peak Strain

The strain values corresponding to the peak stress in the stress–strain curve in Figure 2 were sorted, and the strain under the peak stress of samples with different recycled aggregate contents under the corresponding particle gradations (hereinafter referred to as the peak strain) is shown in Table 6.

Table 6. Peak strain of samples with different content of recycled aggregate/%.

Curing Age	Sample								
	RA-10	RA-20	RA-30	SRA-10	SRA-20	SRA-30	TRA-10	TRA-20	TRA-30
7 d	1.29	1.34	1.26	1.25	1.33	1.21	1.24	1.28	1.24
28 d	1.20	1.24	1.16	1.21	1.26	1.19	1.09	1.23	1.07

It can be seen from Table 6 that the peak strains of samples with different recycled aggregate contents under three particle gradations were kept between 1% and 2%. Therefore, it can be considered that the effect of recycled aggregate content on the peak strain is relatively small. Comparing the peak strains of samples with different curing ages, it can be found that the peak strains of RA-28d, SRA-28d, and TRA-28d samples are all smaller than those of SRA-7d, TRA-7d, and RA-7d samples. As the curing age increases, the cement hydration reaction and pozzolanic reaction of nano-MgO are more complete, which reduces the ductility of samples during loading and makes the samples more prone to brittle failure. Furthermore, it was found that at 7 and 28 d, with the increase in the recycled aggregate content, the peak strain of samples first increased and then decreased, and reached the maximum when the recycled aggregate content was 20%, followed by 10% content, and decreased to the minimum value when the content was 30%. This finding is consistent with the variation law of the peak strength of samples.

3.5. Brittleness Index

According to the above analysis, the variation law of the peak strain of samples was obtained, which can indicate the ductility of samples during the loading process. In order to further determine the brittleness degree of samples when they are damaged, the brittleness index based on the full stress–strain curve [28,29] was introduced, as calculated using Equation (1). The closer the brittleness index to 1, the worse the plasticity of the material.

$$I = 1 - \frac{q_r}{q_u} \quad (1)$$

where I represents the brittleness index; q_u represents the peak strength, kPa; q_r represents the residual strength, kPa.

The brittleness index of samples calculated by the above formula is shown in Table 7.

Table 7. Brittleness index of samples with different contents of recycled aggregate.

Curing Age	Sample								
	RA-10	RA-20	RA-30	SRA-10	SRA-20	SRA-30	TRA-10	TRA-20	TRA-30
7 d	0.987	0.969	0.986	0.983	0.972	0.997	0.992	0.975	0.957
28 d	0.996	0.995	0.995	0.997	0.984	0.998	0.996	0.985	0.970

Table 7 shows that with the increase in curing age, the brittleness index of samples under three particle gradations increases, indicating that the longer the curing age, the

easier the brittle failure of samples occurs. The brittleness index of RA and SRA samples first decreased and then increased with the increase in the recycled aggregate content, and reached the minimum with 20% content. By comparison, the brittleness index of TRA samples decreased with the increase in recycled aggregate content and reached the minimum with 30% content. It is observed that the degree of brittle failure of samples under three particle gradations is highly consistent with the variation law of residual strength, which shows that, to a certain extent, the brittleness index can also represent the ability of samples to resist external loads after failure.

3.6. Initial Elastic Modulus

The initial elastic modulus, E_0 , is one of the important parameters used to describe the deformation of samples. The initial elastic modulus was calculated by formula (2), and the specific numerical change in the initial elastic modulus of samples was obtained as shown in Figure 7. In Equation (2), E_0 represents the initial elastic modulus; $\sigma(\varepsilon)$ represents the stress value under a certain strain, kPa; ε represents the strain, %.

$$E_0 = \frac{d\sigma(\varepsilon)}{d\varepsilon}(\varepsilon = 0) \quad (2)$$

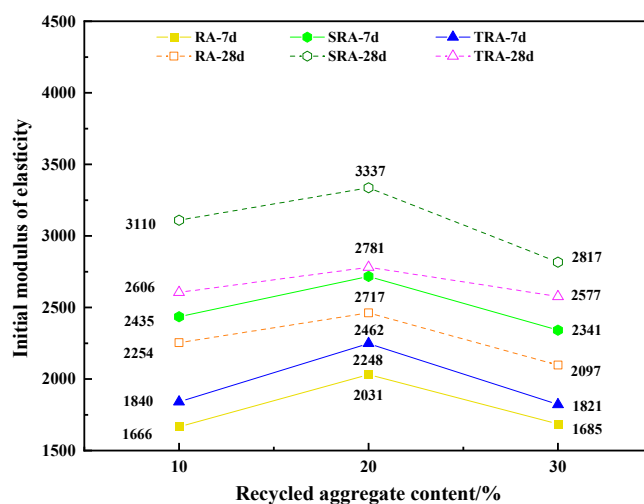


Figure 7. Variation curve of initial elastic modulus of samples with different particle grading recycled aggregate contents.

Figure 7 shows that the initial elastic modulus of RA-28d, SRA-28d, and TRA-28d samples are all higher than those of RA-7d, SRA-7d, and TRA-7d samples with three recycled aggregate contents, indicating that the increase in curing age can improve the ability of samples to resist deformation to a certain extent. At 7 and 28 d, the initial elastic modulus values of RA, SRA, and TRA samples first increased and then decreased with the increase in recycled aggregate content. When the recycled aggregate content was 20%, the initial elastic modulus reached the maximum value, indicating that the sample had the best ability to resist deformation and the highest stiffness. Furthermore, the comparison of the initial elastic modulus of the three particle graded samples shows that at 7 and 28 d, SRA samples show the best resistance to deformation, followed by TRA and, finally, RA.

3.7. Porosity

The recycled aggregate particle gradation mainly affects the pore filling of samples. In order to further determine the compactness of the three particle graded samples of RA, SRA, and TRA, SEM tests were conducted with 20% recycled aggregate content at 7 and

28 d. SEM images under the magnification of 500 times and 2000 times were obtained. Figure 8 shows the SEM images of RA samples magnified 500 times and 2000 times.

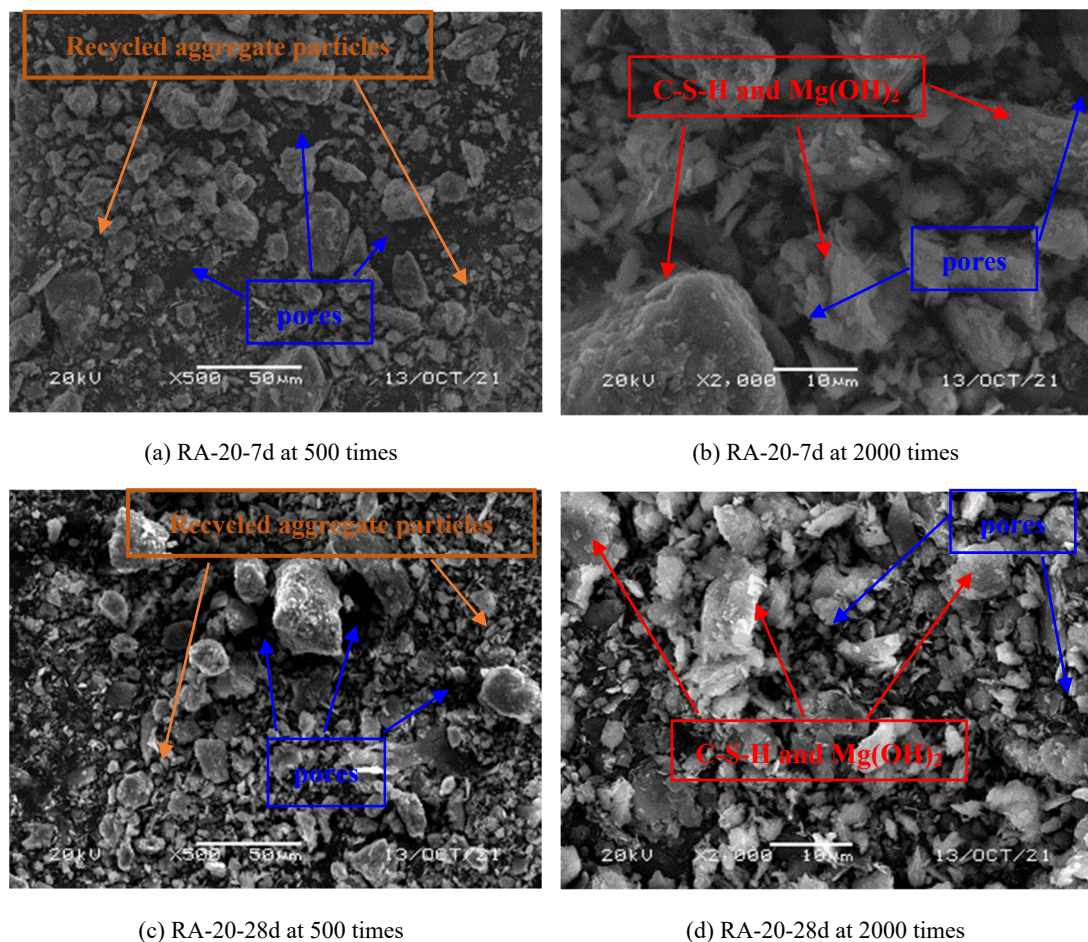


Figure 8. SEM images of RA samples: (a) RA-20-7d at 500 times; (b) RA-20-7d at 2000 times; (c) RA-20-28d at 500 times; (d) RA-20-28d at 2000 times.

Through the four SEM images in Figure 8, the microstructure changes of RA samples at two ages can be further analyzed. At 500 times magnification, it can be clearly seen in Figure 8a that there are a large number of pores in the sample, and the shape of recycled aggregate particles is very obvious. There is a certain interval between particles and the connection is not tight, and the number of pores of the sample in Figure 8c is relatively low compared with that in Figure 8a. The arrangement of recycled aggregate particles is dense and the connection between particles is strengthened. The overall structure is improved. Under the 2000 times magnification, Figure 8b shows the hydration products C-S-H and Mg(OH)₂ of cement and nano-MgO in the RA sample. The hydration products wrap the recycled aggregate particles together, which enhances the bonding between the loose recycled aggregate particles and makes the overall structure of the sample more complete. However, the larger pores in the sample can still be seen. In Figure 8d, the hydration products C-S-H and Mg(OH)₂ are widely dispersed. There are only small pores in the sample, and the overall structure is relatively compact. To summarize, the overall structure of RA samples at the age of 28 d is more compact than that at the age of 7d, and the number and size of pores are reduced. It can thus be proved that the unconfined compressive strength of samples increases with the increase in age.

In order to better analyze the pore structure of the samples, further binarization processing was carried out to convert the SEM images into black and white binarized images by threshold segmentation, as shown in Figure 9. The microscopic image of the soil

is composed of soil particles and pores. It is generally considered that the light-colored areas are soil particles and the dark-colored areas are pores. Therefore, in the binarization process, the soil particles are recorded as white, and the pores are recorded as black, according to which the porosity of samples is calculated [30,31]. The porosity was calculated according to the percentage of the area of the black part in the black and white binarized image to the entire image area, and the specific calculation formula can be expressed as in Equation (3):

$$p = \frac{A_p}{A_t} \times 100\% \quad (3)$$

where p represents the porosity, A_p represents the total area of pores in the black and white binarized image (μm^2), and A_t represents the total area of the black and white binarized image (μm^2). The porosity of the particle gradation samples was calculated as shown in Table 8.

Table 8. Porosity of RA, SRA, and TRA samples/%.

Sample	7d			28d		
	×500	×2000	Weighted Average	×500	×2000	Weighted Average
RA	12.1	13.3	12.3	9.3	10.5	9.5
SRA	4.2	5.5	4.5	3.4	3.5	3.4
TRA	8.1	9.2	8.3	6.6	7.2	6.7

It can be seen from Figure 9 that RA, SRA, and TRA samples at 7 d have more pores than those at 28 d. Furthermore, in the black and white binarized image magnified 2000 times, it can be seen that the pores of samples at 7 d are denser and there are a large number of pores having larger diameters, whereas the pores of samples at the 28 d are relatively small and more widely distributed. In addition, SRA samples have the smallest porosity, followed by TRA samples, and RA samples have the largest porosity.

It can be analyzed from Table 6 that the porosity of the three particle graded samples decreases with the increase in curing age. This is mainly due to the hydration reaction of cement and the pozzolanic reaction of nano-MgO at 28 d, in which more reaction products fill the pores, resulting in a decrease in the porosity of samples. In descending order, the porosity of the three particle graded samples is ranked: SRA, TRA, RA. The results were compared with the compressive strength in the above mechanical tests. It was found that the smaller the porosity, the higher the compressive strength, indicating that the fewer pores in the sample, the tighter the sample structure, and the stronger the bearing capacity of the sample.

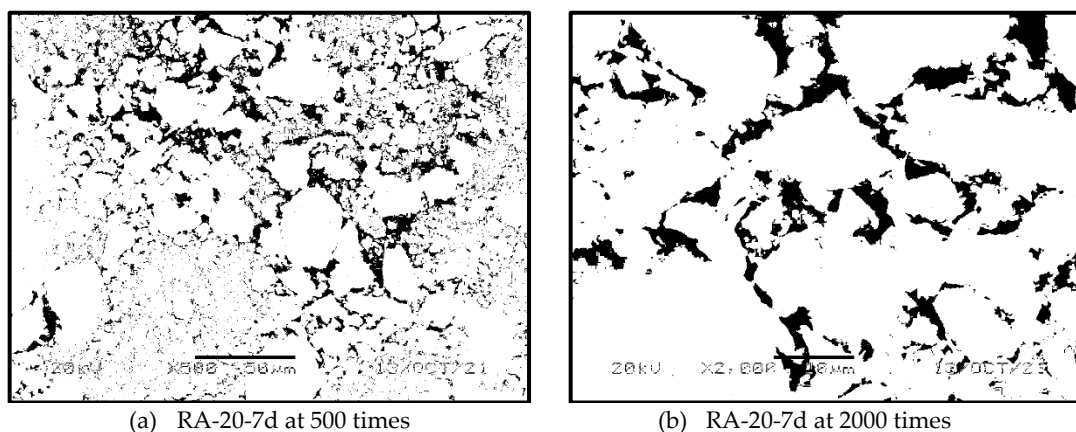
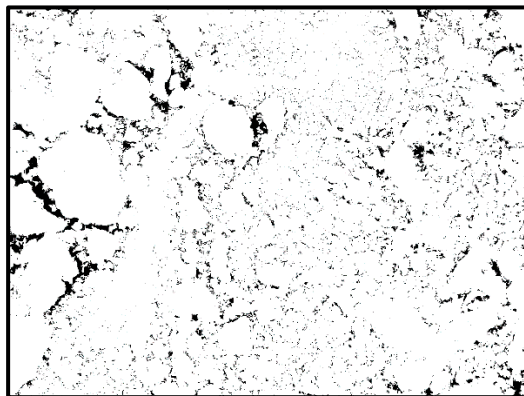
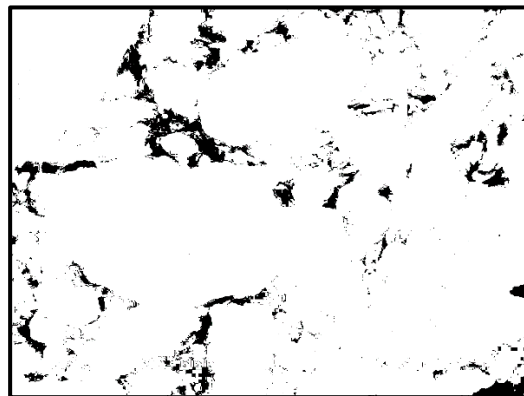


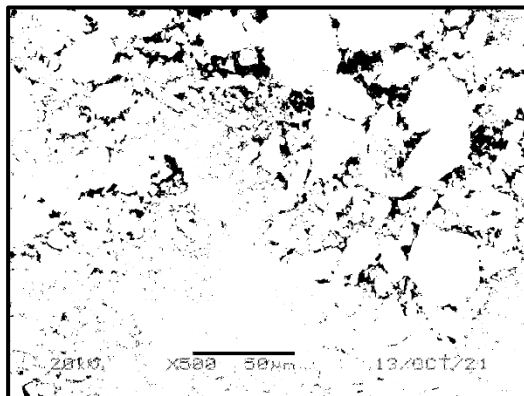
Figure 9. Cont.



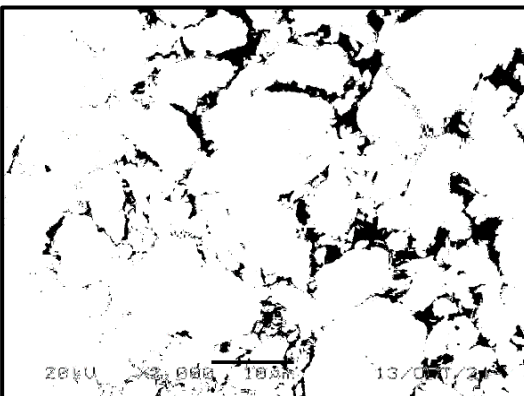
(c) SRA-20-7d at 500 times



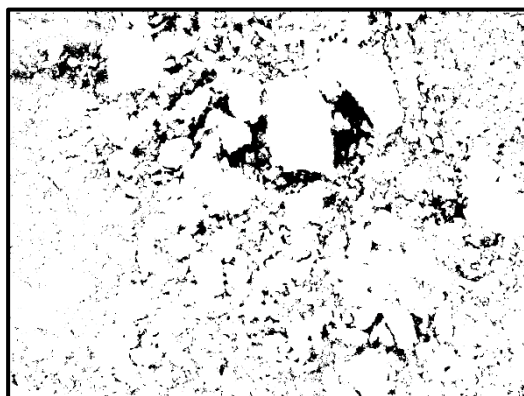
(d) SRA-20-7d at 2000 times



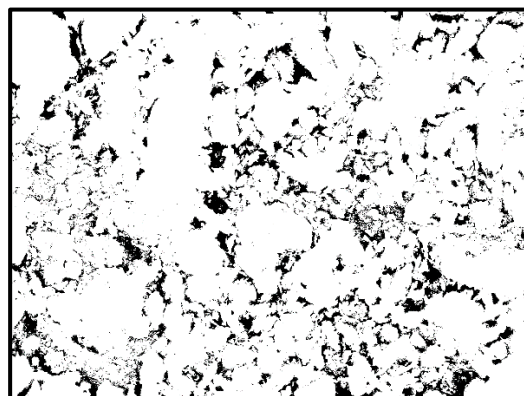
(e) TRA-20-7d at 500 times



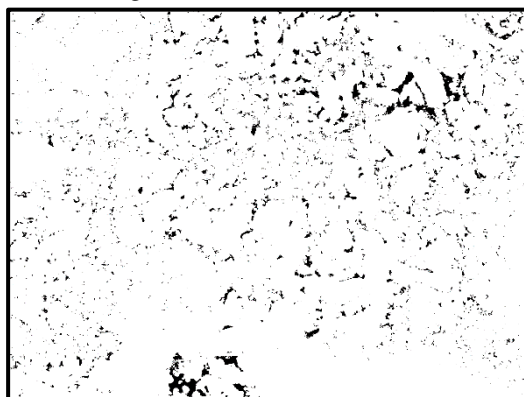
(f) TRA-20-7d at 2000 times



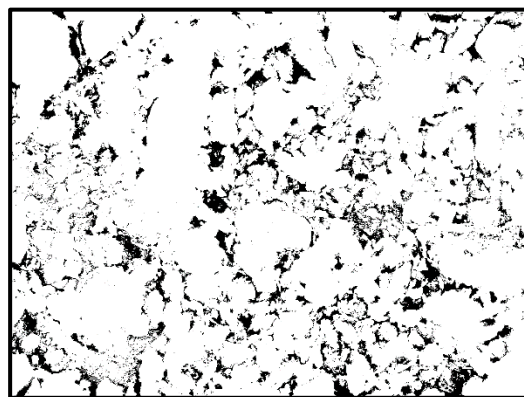
(g) RA-20-28d at 500 times



(h) RA-20-28d at 2000 times



(i) SRA-20-28d at 500 times



(j) SRA-20-28d at 2000 times

Figure 9. Cont.

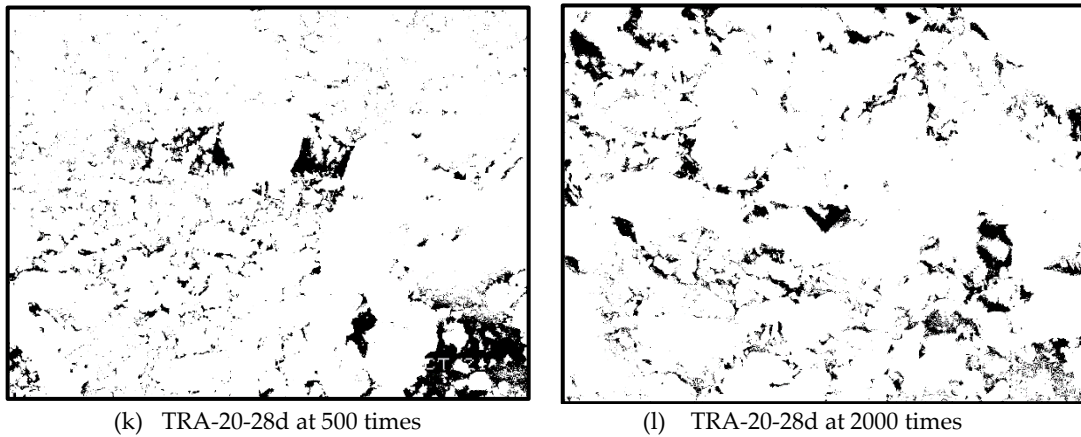


Figure 9. Black and white binary images of RA, SRA, and TRA samples: (a) RA-20-7d at 500 times; (b) RA-20-7d at 2000 times; (c) SRA-20-7d at 500 times; (d) SRA-20-7d at 2000 times; (e) TRA-20-7d at 500 times; (f) TRA-20-7d at 2000 times; (g) RA-20-28d at 500 times; (h) RA-20-28d at 2000 times; (i) SRA-20-28d at 500 times; (j) SRA-20-28d at 2000 times; (k) TRA-20-28d at 500 times; (l) TRA-20-28d at 2000 times.

The porosity of samples when magnified 500 times is lower than that when magnified 2000 times. This is because the sample range involved in SEM images magnified 500 times is larger than that for images magnified 2000 times, and the corresponding porosity decreases. Therefore, the weighted porosity of WPRA samples can be calculated from this. The weight number of porosity for 500 times magnification was set to 4, and that for 2000 times magnification was set to 1, and the final calculation results are listed in Table 8. In order to further study the relationship between the compressive strength and the porosity of RA, SRA, and TRA samples, linear fitting was carried out to obtain their mathematical relationship, as shown in Equation (4), and the fitting curve is drawn as shown Figure 10. It can be seen from the fitting results that the unconfined compressive strength of the samples has a negative exponential power function relationship with porosity.

$$q_u = 6084p^{-0.322} \quad (4)$$

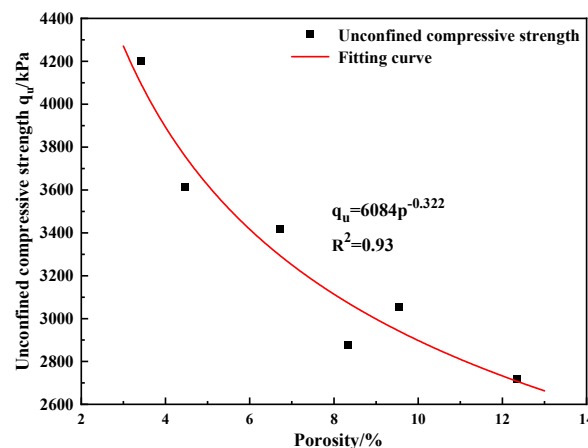


Figure 10. Fitting curve of unconfined compressive strength and porosity.

4. Conclusions

1. The unconfined compressive strengths of RA, SRA, and TRA samples first increase and then decrease with the increase in recycled aggregate content. The unconfined compressive strengths reach the maximum value when the recycled aggregate content is 20%. The unconfined compressive strengths of RA-7d, RA-28d, SRA-7d, SRA-28d,

TRA-7d, and TRA-28d reach 2721, 3053, 3613, 4204, 2878, and 3421kPa, respectively. Compared with the sample with 10% recycled aggregate content, the unconfined compressive strength is improved by between 10% and 30%.

2. Under the three particle gradations, the unconfined compressive strength of SRA samples is the highest, followed by that of TRA, and that of RA is the lowest. At the same curing age and with the same recycled aggregate content, the unconfined compressive strength of SRA samples is stable, and between 20% and 30% higher than that of TRA samples, and between 30% and 40% higher than that of RA samples.
3. The residual strength of both RA and SRA samples reaches the maximum value when the recycled aggregate content is 20%, whereas the residual strength of TRA samples reaches the maximum value when the content is 30%. The variation laws of the peak strain and peak strength of the three particle gradation samples are consistent, and the variation law of the brittle failure degree is highly consistent with that of the residual strength. The initial elastic modulus of all samples first increases and then decreases with the increase in recycled aggregate content. The deformation resistance of the SRA samples is the highest, followed by that of TRA, and that of RA is the lowest.
4. In descending order, the porosity of the three particle graded samples is ranked: SRA, TRA, and RA. The smaller the porosity, the tighter the structure and the stronger the bearing capacity. The compressive strength of the samples has a negative exponential power function relationship with porosity.

Author Contributions: Formal analysis, H.T. and W.W.; writing—review and editing, B.L. and P.J.; investigation, Y.W. and M.D.; conceptualization, Y.P. and N.L. All authors have read and agreed to the published version of the manuscript.

Funding: Zhejiang Provincial Natural Science Foundation of China (Grant number LQ20E080042), the Open Research Fund of State Key Laboratory of Geomechanics and Geotechnical Engineering, Institute of Rock and Soil Mechanics, Chinese Academy of Science (Grant number Z017013) and the Scientific Research Projects of Zhejiang Department of Housing and Urban and Rural Construction of China (Grant number 2017K179, 2019K171).

Institutional Review Board Statement: Not applicable.

Informed Consent Statement: Not applicable.

Data Availability Statement: The data presented in this study are available on request from the corresponding author.

Conflicts of Interest: The authors declare no conflict of interest.

References

1. Zhao, C.H.; Zhao, D. Application of construction waste in the reinforcement of soft soil foundation in coastal cities. *Environ. Technol. Inno.* **2021**, *21*, 101195. [[CrossRef](#)]
2. Yao, J.L.; Qiu, H.J.; He, H.; Chen, X. Application of a Soft Soil Stabilized by Composite Geopolymer. *J. Perform. Constr. Fac.* **2021**, *35*, 04021018. [[CrossRef](#)]
3. Jiang, N.; Wang, C.M.; Wang, Z.P.; Li, B.L.; Liu, Y.A. Strength characteristics and microstructure of cement stabilized soft soil admixed with silica fume. *Materials* **2021**, *14*, 1929. [[CrossRef](#)]
4. Wang, Y.; Zheng, J.L.; You, F. Review on enhancement methods of recycled aggregate. *Mater. Rep.* **2021**, *35*, 5053–5061.
5. Wang, Y.G.; Hughes, P.; Niu, H.C.; Fan, Y.H. A new method to improve the properties of recycled aggregate concrete: Composite addition of basalt fiber and nano-silica. *J. Clean. Prod.* **2019**, *236*, 117602. [[CrossRef](#)]
6. Akhtar, A.; Sarmah, A.K. Construction and demolition waste generation and properties of recycled aggregate concrete: A global perspective. *J. Clean. Prod.* **2018**, *186*, 262–281. [[CrossRef](#)]
7. Xiao, J.; Wang, C.; Ding, T.; Akbarnezhad, A. A recycled aggregate concrete high-rise building: Structural performance and embodied carbon footprint. *J. Clean. Prod.* **2018**, *199*, 868–881. [[CrossRef](#)]
8. Zhang, Y.R.; Luo, W.; Wang, J.J.; Wang, Y.F.; Xu, Y.Q.; Xiao, J.Z. A review of life cycle assessment of recycled aggregate concrete. *Constr. Build. Mater.* **2019**, *209*, 115–125. [[CrossRef](#)]
9. Ahmed, H.; Tiznobaik, M.; Huda, S.B.; Islam, M.S.; Alam, M.S. Recycled aggregate concrete from large-scale production to sustainable field application. *Constr. Build. Mater.* **2020**, *262*, 119979. [[CrossRef](#)]

10. Liu, F.; Lin, X.; Wang, J. Influence of particle-size gradation on shear behavior of geosynthetics and sand interface. *Chin. J. Rock Mech. Eng.* **2013**, *32*, 2575–2582.
11. Liu, Y.J.; Li, G.; Yin, Z.Y.; Xia, X.H.; Wang, J.H. Influence of grain gradation on undrained mechanical behavior of granular materials. *Rock Soil Mech.* **2015**, *36*, 423–429.
12. Mollamahmutoglu, M.; Avci, E. Effects of Particle Gradation, Relative Density and Curing on the Strength of Silicate Grouted Sand. *Geotech. Geol. Eng.* **2020**, *38*, 6695–6715. [[CrossRef](#)]
13. Chian, S.C.; Bi, J. Influence of grain size gradation of sand impurities on strength behaviour of cement-treated clay. *Acta Geotech.* **2021**, *16*, 1127–1145. [[CrossRef](#)]
14. Huang, Y.T.; Wang, J.; Ying, M.J.; Ni, J.F.; Li, M.F. Effect of particle-size gradation on cyclic shear properties of recycled concrete aggregate. *Constr. Build. Mater.* **2021**, *301*, 124143. [[CrossRef](#)]
15. Ren, Y.B.; Wang, Y.; Yang, Q. Effects of particle size distribution and shape on permeability of calcareous sand. *Rock Soil Mech.* **2018**, *39*, 491–497.
16. Xie, K.Z.; Liu, Z.W.; Zheng, K.X.; Ge, B.Z.; Xin, Y. Research on the properties of manufactured sand concrete with different grain composition. *Concrete* **2021**, *4*, 91–95.
17. Duan, Z.H.; Li, B.; Xiao, J.Z.; Guo, W. Optimizing mix proportion of recycled aggregate concrete by readjusting the aggregate gradation. *Struct. Concr.* **2021**, *22*, E22–E32. [[CrossRef](#)]
18. Li, B.; Hou, S.D.; Duan, Z.H.; Li, L.; Guo, W. Rheological behavior and compressive strength of concrete made with recycled fine aggregate of different size range. *Constr. Build. Mater.* **2021**, *268*, 121172. [[CrossRef](#)]
19. Yao, Y.S.; Li, J.; Liang, C.H.; Hu, X. Effect of Coarse Recycled Aggregate on Failure Strength for Asphalt Mixture Using Experimental and DEM Method. *Coatings* **2021**, *11*, 1234. [[CrossRef](#)]
20. Kaplan, G.; Gulcan, A.; Cagdas, B.; Bayraktar, O.Y. The impact of recycled coarse aggregates obtained from waste concretes on lightweight pervious concrete properties. *Environ. Sci. Pollut. Res.* **2021**, *28*, 17369–17394. [[CrossRef](#)]
21. Revilla-Cuesta, V.; Evangelista, L.; de Brito, J.; Skaf, M.; Ortega-López, V. Mechanical performance and autogenous and drying shrinkage of MgO-based recycled aggregate high-performance concrete. *Constr. Build. Mater.* **2022**, *314*, 125726. [[CrossRef](#)]
22. Peng, W. *Laboratory Investigation on the Effect of Particle Size Distribution on Mechanical Properties of Calcareous Sands Improved by Polyurethane Foam Adhesive*; Hubei University of Technology: Wuhan, China, 2020.
23. China Renewable Energy Engineering Institute. *Standard for Geotechnical Testing Method: GB/T50123-2019*; China Planning Press: Beijing, China, 2019.
24. Li, Y.G.; Ma, X.L.; Hu, D.W.; Kang, Y.H. Influence of aeolian sand content on mechanism of mortar and concrete. *Bull. Chin. Ceramic. Soc.* **2017**, *36*, 2128–2133.
25. Li, F. Experimental analysis of the influence of sand content on the Duncan-Chang model parameters of cement mortar pile. *J. Railw. Sci. Eng.* **2018**, *15*, 645–650.
26. Xu, C.S.; Wang, X.; Lu, X.Y.; Dai, F.C.; Jiao, S. Experimental study of residual strength and the index of shear strength characteristics of clay soil. *Eng. Geol.* **2018**, *233*, 183–190. [[CrossRef](#)]
27. Sadrmomtazi, A.; Gashti, S.H.; Tahmouresi, B. Residual strength and microstructure of fiber reinforced self-compacting concrete exposed to high temperatures. *Constr. Build. Mater.* **2020**, *230*, 116969. [[CrossRef](#)]
28. Bishop, A.W. Shear strength parameters for undisturbed and remoulded soil specimens. In *Proceedings of the Roscoe Memorial Symposium*; Cambridge University: Cambridge, MA, UK, 1971; pp. 29–31.
29. Ta'negonbadi, B.; Noorzad, R. Stabilization of clayey soil using lignosulfonate. *Transp. Geotech.* **2017**, *12*, 45–55. [[CrossRef](#)]
30. Zhang, X.W.; Kong, L.W.; Guo, A.G.; Tuo, Y.F. Evolution of microscopic pore of structured clay in compression process based on SEM and MIP test. *Chin. J. Rock Mech. Eng.* **2012**, *31*, 406–412.
31. Wang, W.; Liu, J.J.; Li, N.; Ma, L. Mechanical properties and micro mechanism of Nano-SiO₂ modified coastal cement soil at short age. *Acta Mater. Compos. Sin.* **2021**, *12*, 1–16.